

# The preparation and properties of $\text{La}_{3.5}\text{Ru}_4\text{O}_{13}$ and $\text{La}_2\text{RuO}_5$

Andreja Benčan\*, Marko Hrovat, Janez Holc, Goran Dražič, Marija Kosec

*Jozef Stefan Institute, Jamova 39, Ljubljana 1000, Slovenia*

Received 11 January 2004; received in revised form 13 April 2004; accepted 22 April 2004

Available online 26 June 2004

## Abstract

The stability of the  $\text{La}_{3.5}\text{Ru}_4\text{O}_{13}$  and  $\text{La}_2\text{RuO}_5$  compounds in the La–Ru–O system in various atmospheres and various temperature ranges was investigated by thermal analysis, X-ray diffraction analysis and electron microscopy. The  $\text{La}_{3.5}\text{Ru}_4\text{O}_{13}$  compound is stable in oxidizing and neutral atmospheres ( $\text{N}_2$  with 10 ppm  $\text{O}_2$ ), while  $\text{La}_2\text{RuO}_5$  is partially reduced in a neutral atmosphere to form  $\text{La}_2\text{RuO}_{4.6}$ . In a reducing atmosphere both compounds decompose into metallic Ru and  $\text{La}_2\text{O}_3$ . The thermal expansion coefficients of  $\text{La}_2\text{RuO}_5$  and  $\text{La}_{3.5}\text{Ru}_4\text{O}_{13}$  at  $800^\circ\text{C}$  are  $11.2 \times 10^{-6} \text{ K}^{-1}$  and  $9.3 \times 10^{-6} \text{ K}^{-1}$ , respectively. The specific electrical resistivity for  $\text{La}_{3.5}\text{Ru}_4\text{O}_{13}$  is relatively independent of temperature and is  $2 \times 10^{-2} \Omega \text{ cm}$  at  $800^\circ\text{C}$ , while for  $\text{La}_2\text{RuO}_5$  it decreases with increasing temperature and is  $1 \Omega \text{ cm}$  at  $800^\circ\text{C}$ .

© 2004 Elsevier Ltd. All rights reserved.

*Keywords:* Ruthenates; Electrical properties; Thermal properties; Fuel cells;  $\text{La}_2\text{RuO}_5$

## 1. Introduction

The operating temperatures of fuel cells with solid oxide electrolytes (SOFC) are around  $1000^\circ\text{C}$ , but the current trend in their development is to lower the operating temperatures to near or under  $800^\circ\text{C}$ . However, the ionic conductivity of yttria-stabilized zirconia (YSZ), which is usually used as the solid electrolyte, decreases by factor of 3 when the temperature is decreased from  $1000$  to  $800^\circ\text{C}$ . To overcome this problem, one way could be to look at other types of ceramic ionic conductors with lower ionic resistivity.  $\text{CeO}_2$  doped with 3+ ions (e.g.,  $\text{Gd}^{3+}$ ) and  $\text{LaGaO}_3$  doped with 2+ ions (on A and B sites with  $\text{Sr}^{2+}$  and  $\text{Mg}^{2+}$ , respectively) are mentioned in the literature as the most suitable “candidates”.<sup>1</sup>

The cathode or air electrode material for an SOFC operating at  $1000^\circ\text{C}$  is mostly based on  $(\text{La}_{1-x}\text{Sr}_x)\text{MnO}_3$ . It is a relatively good electronic conductor with a specific resistivity of  $0.1 \Omega \text{ cm}$  at  $1000^\circ\text{C}$  but its ionic conductivity is low. At lower operating temperatures the polarization losses of manganites become high and the operation efficiency of a SOFC deteriorate.<sup>2</sup> Therefore, other materials with better electrical characteristics are required.

Ruthenium dioxide and many ruthenates are good electrical conductors and useful electro-catalysts for oxygen reduction.<sup>3</sup> One of the potential systems, which could be used as basis for a material for the cathode in a SOFC is the La–Ru–O system. The reactivity studies of lanthanum ruthenates with materials for the solid electrolyte (i.e.,  $\text{LaGaO}_3$ ,  $\text{CeO}_2$ , YSZ) indicated that lanthanum ruthenates are compatible with these electrolytes.<sup>4</sup> According to the literature a variety of phases are possible in the La–Ru–O system, depending on the preparation route and the temperature.

Ten compounds in the mentioned system are described in the open literature.<sup>5–18</sup> The nominal valence of the ruthenium ion varies from 3+<sup>8–10</sup> to 5+.<sup>15–18</sup> Also the specific resistivity varies from  $2.5 \text{ m}\Omega \text{ cm}$  at  $20^\circ\text{C}$  for  $\text{La}_4\text{Ru}_6\text{O}_{19}$ <sup>5,6</sup> to  $>2 \text{ M}\Omega$  at  $20^\circ\text{C}$  for  $\text{La}_7\text{Ru}_3\text{O}_{18}$ .<sup>15</sup> However only four compounds, i.e.,  $\text{La}_{3.5}\text{Ru}_4\text{O}_{13}$ ,<sup>7</sup>  $\text{La}_{4.87}\text{Ru}_2\text{O}_{12}$ ,<sup>15</sup>  $\text{La}_7\text{Ru}_3\text{O}_{18}$ <sup>15</sup> and a recently published  $\text{La}_2\text{RuO}_5$ <sup>12,13</sup> can be prepared by synthesis in air. Others are synthesized either under reducing or strongly oxidizing conditions. Table 1 summarizes the published crystallographic data on the lanthanum ruthenates, including the nominal valence of the ruthenium ions and, when reported, the data on the electrical resistivity.

The aim of this study was to evaluate the thermal stability, the thermal expansion coefficients and the electrical properties of  $\text{La}_2\text{RuO}_5$  and  $\text{La}_{3.5}\text{Ru}_4\text{O}_{13}$  as important properties of possible cathode materials.

\* Corresponding author.

E-mail address: [andreja.bencan@ijs.si](mailto:andreja.bencan@ijs.si) (A. Benčan).

Table 1  
Published crystallographic data and electrical properties of lanthanum ruthenates

Compound	Symmetry	Space group	Nominal Ru valence	Electrical resistivity	Reference
La <sub>4</sub> Ru <sub>6</sub> O <sub>19</sub>	Cubic	<i>I</i> 23 (197)	4.33+	2.5 mΩ cm at 20 °C; $R_{300\text{K}}/R_{1\text{K}} = 192$	5,6
La <sub>3.5</sub> Ru <sub>4</sub> O <sub>13</sub>	Orthorhombic	<i>Pmmm</i> (47)	3.875+	–	7
LaRuO <sub>3</sub>	Orthorhombic	<i>Pnma</i> (62); <i>Pbnm</i> (62)	3+	$5 \times 10^{-3}$ Ω cm (at 20 °C); $1.08 \times 10^{-3}$ Ω cm (at 4.2 K); $1.2 \times 10^{-3}$ Ω cm (at 77 K); $1.74 \times 10^{-3}$ Ω cm (at 300 K)	8–10
La <sub>3</sub> Ru <sub>3</sub> O <sub>11</sub>	Cubic	<i>Pn</i> $\bar{3}$ (201)	4.33+	$R_{300\text{K}}/R_{4\text{K}} = 33$	11
La <sub>2</sub> RuO <sub>5</sub> (La <sub>4</sub> Ru <sub>2</sub> O <sub>10</sub> )	Monoclinic	<i>P</i> 2 <sub>1</sub> / <i>c</i> (14) above 170 K; <i>P</i> $\bar{1}$ (2) below 150 K	4+	$\sim 10^4$ Ω cm (at 166 K); $\sim 10^6$ Ω cm (at 111 K); $\sim 10^2$ Ω cm (at 60 °C)	12,13
La <sub>8</sub> Ru <sub>4</sub> O <sub>21</sub>	Hexagonal	<i>P</i> 6 <sub>3</sub> <i>cm</i> (185)	4.5+	–	14
La <sub>7</sub> Ru <sub>3</sub> O <sub>18</sub>	Trigonal	<i>R</i> $\bar{3}$ <i>cc</i> (167)	5+	>2 MΩ at 20 °C	15
La <sub>4.87</sub> Ru <sub>2</sub> O <sub>12</sub>	Monoclinic	<i>P</i> 2 <sub>1</sub> / <i>c</i> (14)	4.695+	100 kΩ at 20 °C	15
La <sub>3</sub> RuO <sub>7</sub>	Orthorhombic	<i>Cmcm</i> (63)	5+	425 Ω cm at 20 °C	16,17
β-La <sub>3</sub> RuO <sub>7</sub>	Monoclinic	<i>P</i> 2 <sub>1</sub> / <i>c</i> (14)	5+	–	18

The two compounds were chosen as they can be synthesized in air. The other two compounds (La<sub>7</sub>Ru<sub>3</sub>O<sub>18</sub> and La<sub>4.87</sub>Ru<sub>2</sub>O<sub>12</sub>), which can be also synthesized in air, have too high specific resistivity to be considered as electrode materials for SOFC.

## 2. Experimental

The La<sub>3.5</sub>Ru<sub>4</sub>O<sub>13</sub> and La<sub>2</sub>RuO<sub>5</sub> compounds were synthesized from La(OH)<sub>3</sub> (Ventron, 99.9%) and RuO<sub>2</sub> (Ventron, 99.9%) using conventional solid-state synthesis techniques. Stoichiometric amounts of RuO<sub>2</sub> and La(OH)<sub>3</sub> were mixed in isopropyl alcohol, pressed into pellets and fired in air. During firing, the pellets were placed on platinum foils. The samples were fired three times (with intermediate grinding) in air at 1000 and 1150 °C, respectively.

The fired materials were characterized with XRD analysis using a Philips PW 1710 X-ray diffractometer and Cu Kα radiation. The X-ray patterns were measured in the range  $2\theta = 20^\circ - 70^\circ$  using steps of 0.04°. The samples were additionally characterized using a JEOL 5800 scanning electron microscope (SEM) and an analytical electron microscope (JEM 2010F); both microscopes were equipped with a LINK ISIS 300 energy-dispersive X-ray spectrometer. The samples prepared for the SEM were mounted in epoxy and then polished using standard metallographic techniques. Prior to analysis in the SEM, the samples were coated with carbon to provide electrical conductivity and to avoid charging effects.

The samples for transmission electron microscopy (TEM) were prepared by mechanical thinning, dimpling and ion milling using 3.8 keV argon ions. The Cliff–Lorimer method and absorption corrections were employed for the quantitative analysis. La<sub>4.87</sub>Ru<sub>2</sub>O<sub>12</sub> fired at 1000 °C, was used as a standard. The concentration of oxygen was calculated from the stoichiometry.

Simulated electron-diffraction “powder” patterns were calculated using the EMS program package.<sup>19</sup> As a result

of the calculations, a listing of the positions of the powder lines and their intensities was created. The intensities were calculated from the structure factors and corrected using a shape factor that depends on the crystal size. Dynamical effects were not considered in the calculations. To be able to compare the experimental and simulated electron-diffraction patterns, images were constructed from the intensity distributions as described in.<sup>20</sup>

The electrical DC resistance was measured for the as-fired pellets using the four-point method in the temperature range 20–900 °C in air. Fritless Pt electrodes (Demetron M8014), painted on the sintered pellets and fired at 1000 °C, were used for the contacts.

The thermal stability of the prepared compounds was investigated using thermogravimetric analysis (TGA, Netzsch STA 492) in the temperature range 20–800 °C at a heating rate of 10 K/min. The TGA analysis were performed in environments with different oxygen partial pressures (pure oxygen, air and nitrogen (10 ppm O<sub>2</sub>)) and in reducing atmosphere (Ar–10% H<sub>2</sub>). The weight of the samples was around 500 mg.

Additional experiments on thermal stability were done in a furnace with Ar (100 ppm O<sub>2</sub>) atmosphere heated up to 1250 °C.

The thermal expansion measurements were carried out from room temperature to 800 °C using a dilatometer (DIL 802, Bähr Germany) with a constant heating rate of 10 K/min in air.

## 3. Results and discussion

### 3.1. The La<sub>3.5</sub>Ru<sub>4</sub>O<sub>13</sub> compound

The La<sub>3.5</sub>Ru<sub>4</sub>O<sub>13</sub> compound, which crystallizes in an orthorhombic unit cell,<sup>7</sup> was synthesized by firing for 10 h at 1000 °C. Fig. 1 shows the high-temperature X-ray diffraction patterns of La<sub>3.5</sub>Ru<sub>4</sub>O<sub>13</sub> in air. In the temperature range

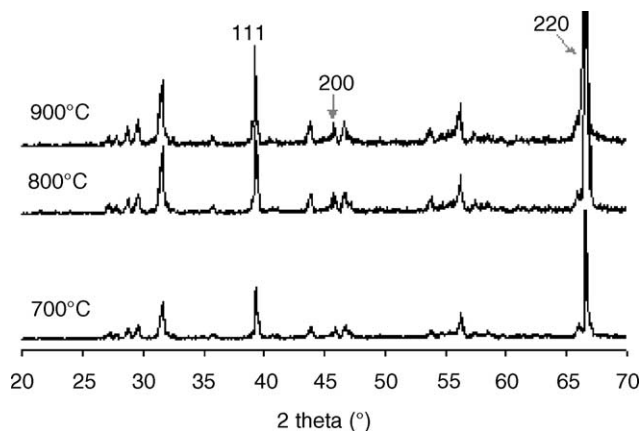
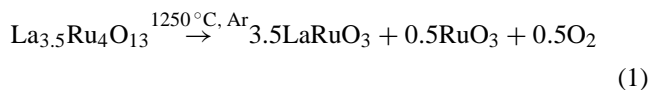


Fig. 1. High-temperature X-ray diffraction patterns of  $\text{La}_{3.5}\text{Ru}_4\text{O}_{13}$  in the temperature range 700–900 °C. Peaks denoted as [1 1 1], [2 0 0] and [2 2 0] originate from the Pt sample holder in the X-ray diffractometer.

700–900 °C no phase transitions were detected. The additional reflections originate from the Pt sample holder in the X-ray diffractometer.

The TGA measurements of  $\text{La}_{3.5}\text{Ru}_4\text{O}_{13}$  in oxygen, air and nitrogen (10 ppm  $\text{O}_2$ ) from room temperature to 800 °C did not show any detectable weight change indicating the stability of this compound in oxidizing and neutral atmospheres.

Fig. 2 shows the X-ray pattern of  $\text{La}_{3.5}\text{Ru}_4\text{O}_{13}$  after firing at 1250 °C, 2 h in Ar (100 ppm  $\text{O}_2$ ). X-ray peaks show that, after firing in Ar atmosphere, peaks of  $\text{La}_{3.5}\text{Ru}_4\text{O}_{13}$  disappear and the perovskite  $\text{LaRuO}_3$  is formed. Presumably, during the firing at 1250 °C, oxygen and ruthenium (in the form of  $\text{RuO}_3^{21}$ ) evaporate according to (Eq. (1)):



After firing at 800 °C in a reducing atmosphere (Ar–10%  $\text{H}_2$ ),  $\text{La}_{3.5}\text{Ru}_4\text{O}_{13}$  decomposed into metallic Ru and  $\text{La}_2\text{O}_3$  (Eq. (2)). In Fig. 3 X-ray peaks denoted as Ru belong to metallic Ru, while the others are attributed to  $\text{La}(\text{OH})_3$ .  $\text{La}_2\text{O}_3$  reacts with  $\text{H}_2\text{O}$  from the air and forms  $\text{La}(\text{OH})_3$ .

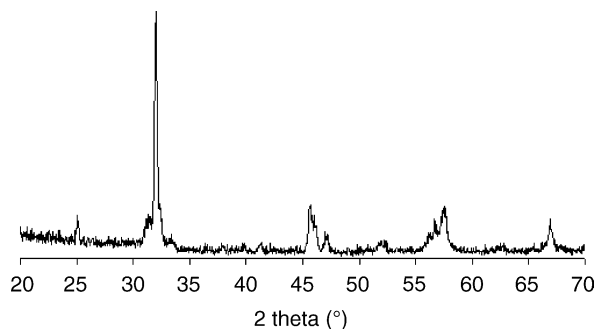


Fig. 2. X-ray pattern of  $\text{La}_{3.5}\text{Ru}_4\text{O}_{13}$  after firing at 1250 °C in Ar (100 ppm  $\text{O}_2$ ). All peaks can be indexed with the  $\text{LaRuO}_3$  perovskite unit cell (ICDD-PDF: 82-1477).

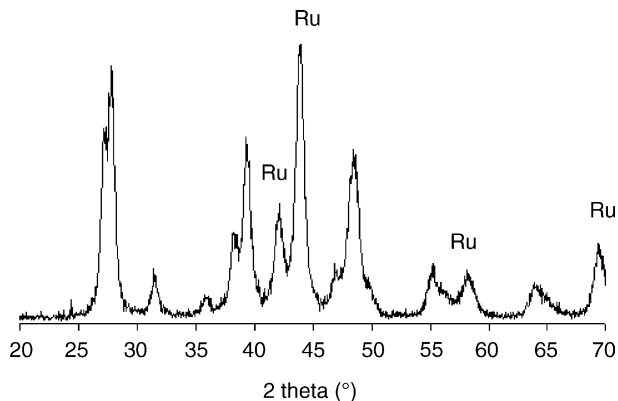


Fig. 3. XRD pattern of the  $\text{La}_{3.5}\text{Ru}_4\text{O}_{13}$  after firing at 800 °C in a reducing atmosphere (Ar–10%  $\text{H}_2$ ). Peaks denoted as “Ru” belong to metallic Ru, others are attributed to  $\text{La}(\text{OH})_3$ .

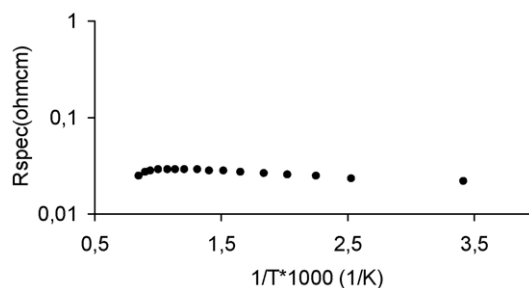
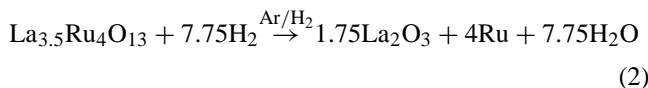


Fig. 4. The specific resistivity vs. reciprocal temperature for  $\text{La}_{3.5}\text{Ru}_4\text{O}_{13}$ , measured in air.



The specific resistivities versus reciprocal temperature for the  $\text{La}_{3.5}\text{Ru}_4\text{O}_{13}$  are presented in Fig. 4. The resistivity of  $\text{La}_{3.5}\text{Ru}_4\text{O}_{13}$  is relatively independent of temperature throughout the whole measured temperature range. The room-temperature resistivity of  $\text{La}_{3.5}\text{Ru}_4\text{O}_{13}$ , as well as the resistivity at 800 °C, is around  $2 \times 10^{-2} \Omega \text{ cm}$  in air.

Fig. 5 shows the temperature dependence of the thermal expansion of  $\text{La}_{3.5}\text{Ru}_4\text{O}_{13}$ . The thermal expansion coefficients (TECs) are tabulated in Table 2.

### 3.2. The $\text{La}_2\text{RuO}_5$ compound

The  $\text{La}_2\text{RuO}_5$  compound was synthesized by firing for 15 h at 1150 °C. Fig. 6 shows TGA measurements of  $\text{La}_2\text{RuO}_5$  from room temperature to 800 °C in air, in oxygen

Table 2  
The values of the expansion coefficients of  $\text{La}_{3.5}\text{Ru}_4\text{O}_{13}$

Temperature region (°C)	TEC $\times 10^{-6} (\text{K}^{-1})$ [ $\text{La}_{3.5}\text{Ru}_4\text{O}_{13}$ ]
Room temperature–270	7.4
270–520	7.4–8.5
520–800	8.5–9.3

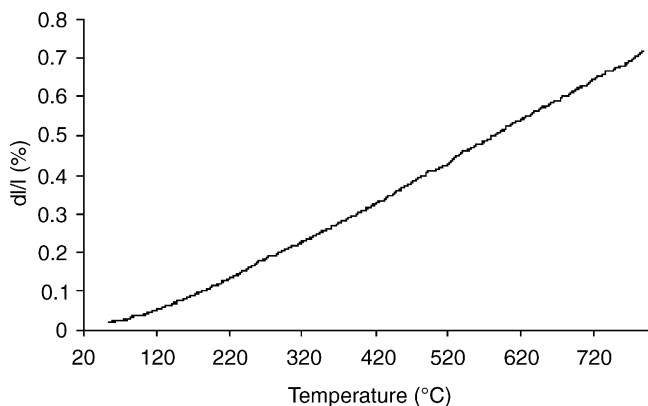
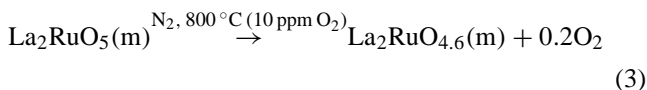


Fig. 5. Temperature dependence of the thermal expansion of  $\text{La}_{3.5}\text{Ru}_4\text{O}_{13}$ .

and in  $\text{N}_2$ . According to the TGA measurements,  $\text{La}_2\text{RuO}_5$  is stable in oxygen. In air, a small weight loss of around 0.1 wt.% was observed at  $800^\circ\text{C}$ . However, in the neutral atmosphere ( $\text{N}_2$  with 10 ppm  $\text{O}_2$ ) a weight loss of 1.5% was observed at  $600^\circ\text{C}$ . It was presumed that the weight loss is due only to the loss of oxygen, as the evaporation of volatile  $\text{RuO}_3$  and  $\text{RuO}_4$  compounds is negligible at temperatures under  $1000^\circ\text{C}$ .<sup>21</sup> This indicates that  $\sim 4/5$   $\text{Ru}^{4+}$  in  $\text{La}_2\text{RuO}_5$  is reduced to  $\text{Ru}^{3+}$  forming the substoichiometric compound with the nominal composition  $\text{La}_2\text{RuO}_{4.6}$  (or  $\text{La}_{10}(\text{Ru}^{3+})_4(\text{Ru}^{4+})\text{O}_{23}$ ) (Eq. (3)):



The X-ray patterns of the  $\text{La}_2\text{RuO}_5$  compound and the partially reduced  $\text{La}_2\text{RuO}_{4.6}$  compound are shown in Fig. 7. A small decrease in the size of the  $a$  and  $b$  unit-cell parameters of  $\text{La}_2\text{RuO}_5$  was observed after firing in inert atmosphere (Table 3). However, the unit cell of the substoichiometric  $\text{La}_2\text{RuO}_{4.6}$  compound is still monoclinic— $P2_1/c$ .<sup>12</sup>

The TGA analysis of  $\text{La}_2\text{RuO}_5$  in  $\text{Ar}/10\%\text{H}_2$  is shown in Fig. 8. The TGA curve shows a weight loss of around 1.5%

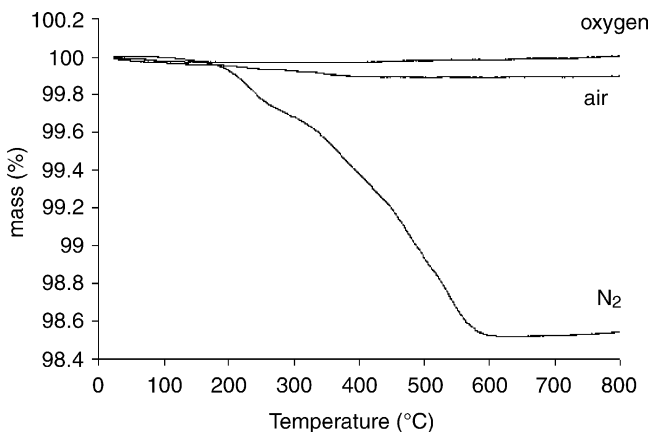


Fig. 6. TGA measurements of  $\text{La}_2\text{RuO}_5$  in air, in oxygen and in  $\text{N}_2$  (10 ppm  $\text{O}_2$ ) up to  $800^\circ\text{C}$ .

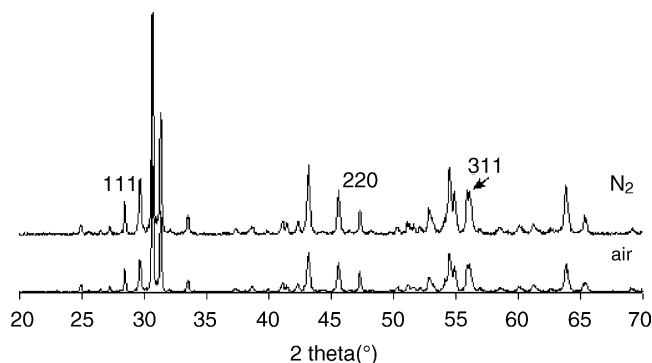


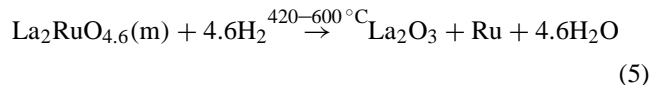
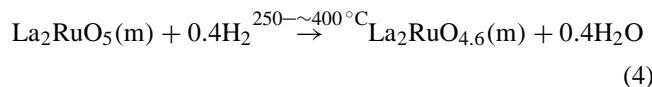
Fig. 7. XRD pattern of  $\text{La}_2\text{RuO}_5$  after TGA analysis in air and in  $\text{N}_2$ . The additional peaks denoted as [1 1 1], [2 2 0] and [3 1 1] originate from Si, which was added as an internal standard.

Table 3

Cell parameters of  $\text{La}_2\text{RuO}_5$  and  $\text{La}_2\text{RuO}_{4.6}$ , monoclinic unit cell,  $P2_1/c$

Cell parameters	$\text{La}_2\text{RuO}_5$	$\text{La}_2\text{RuO}_{4.6}$
$a$ (Å)	9.1955	9.1830
$b$ (Å)	5.8344	5.8330
$c$ (Å)	7.9601	7.9636
$\beta$ (°)	100.773	100.773
$V$ (Å <sup>3</sup> )	419.53	419.05

between  $250$  and  $400^\circ\text{C}$ , and a further weight loss of 5.4% between  $420$  and  $620^\circ\text{C}$ . The first loss is ascribed to the formation of the partially reduced  $\text{La}_2\text{RuO}_{4.6}$  ruthenate, while the total weight loss ( $\sim 6.9\%$ ) corresponds to the reduction of  $\text{La}_2\text{RuO}_5$  to metallic Ru and  $\text{La}_2\text{O}_3$  (Eqs. (4) and (5)):



Since with XRD only the  $\text{La}(\text{OH})_3$  (due to the reaction of  $\text{La}_2\text{O}_3$  with  $\text{H}_2\text{O}$ ) was identified the assumption was that

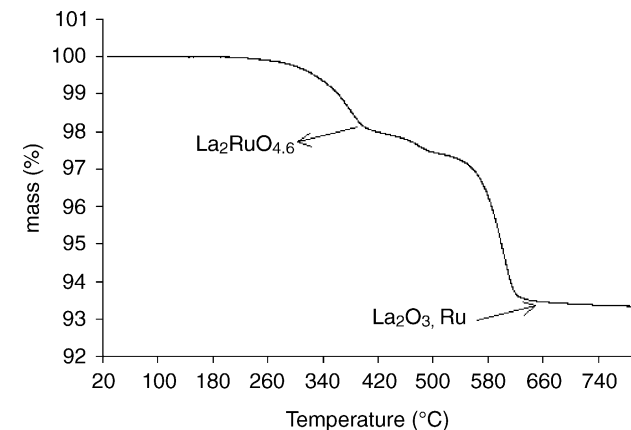


Fig. 8. TGA measurement of  $\text{La}_2\text{RuO}_5$  in reducing atmosphere up to  $800^\circ\text{C}$ .

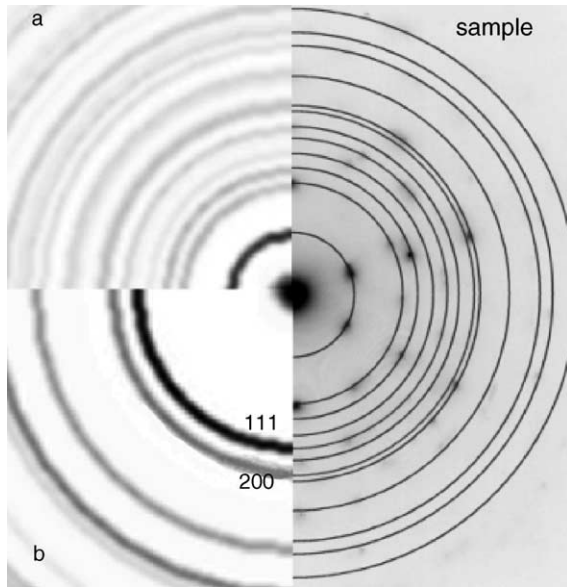


Fig. 9. Experimental SAED pattern of  $\text{La}_2\text{RuO}_5$ , after firing in a reducing atmosphere. Simulated patterns of  $\text{La}(\text{OH})_3$  (a) and cubic Ru (b) are added. SAED pattern of the sample can be indexed with  $\text{La}(\text{OH})_3$  and with [1 1 1], [2 0 0] rings of metallic Ru.

the peaks of metallic Ru in the sample could not be detected due to a particle size in the nanometer range. In order to determine the Ru and  $\text{La}(\text{OH})_3$  in the sample, analytical electron microscopy was used after TG measurement in the reducing atmosphere. Instead of measuring the  $d$  values, experimental selected-area electron-diffraction (SAED) patterns were compared to the calculated patterns. For the simulations, published crystal-structure data for  $\text{La}(\text{OH})_3$  (PDF: 83-2034) and metallic Ru (PDF: 88-2333) were used. The electron diffraction patterns for a mean crystallite size between 0.5 and 5 nm were systematically calculated.

Fig. 9 shows the experimental SAED pattern of  $\text{La}_2\text{RuO}_5$  after firing in a reducing atmosphere. The simulated diffraction patterns of  $\text{La}(\text{OH})_3$  (a) and cubic Ru (b) with 5 nm particle sizes are added. Based on the comparison of the experimental SAED patterns with the simulated patterns it was found that the faint rings in the SAED patterns indicate a presence of  $\text{La}(\text{OH})_3$  with a grain size around 10 nm and of metallic Ru with a grain size of a few nanometers.

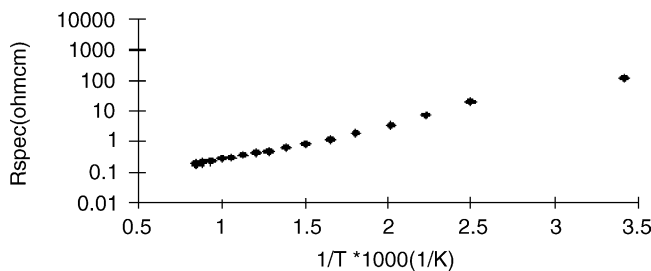


Fig. 10. The logarithm of specific resistivities vs. reciprocal temperature for  $\text{La}_2\text{RuO}_5$  in air.

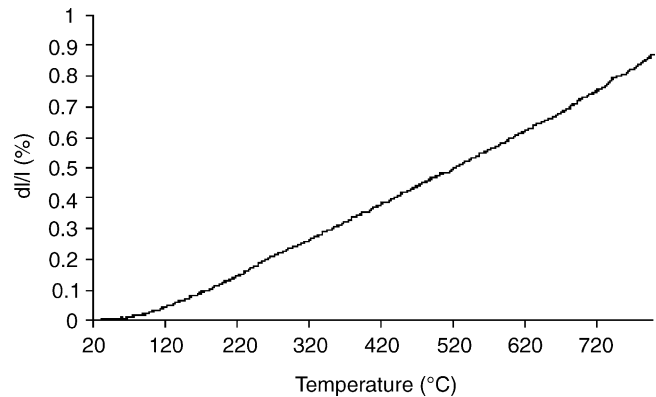


Fig. 11. Temperature dependence of the thermal expansion of  $\text{La}_2\text{RuO}_5$ .

Table 4

The values of the expansion coefficients of  $\text{La}_2\text{RuO}_5$

Temperature region (°C)	TEC $\times 10^{-6}$ ( $\text{K}^{-1}$ ) [ $\text{La}_2\text{RuO}_5$ ]
Room temperature–270	8.4
270–520	8.4–9.9
520–800	9.9–11.2

The logarithm of specific resistivities versus reciprocal temperature for  $\text{La}_2\text{RuO}_5$  is presented in Fig. 10. The specific resistivity of  $\text{La}_2\text{RuO}_5$  decreases with increasing temperature from 115  $\Omega$  cm at 20 °C to around 1  $\Omega$  cm at 800 °C. This semiconducting behaviour of  $\text{La}_2\text{RuO}_5$  is in agreement with the results recently published by Khalifah et al.<sup>13</sup>

Fig. 11 shows the temperature dependence of the thermal expansion of  $\text{La}_2\text{RuO}_5$ . The thermal expansion coefficients (TECs) are tabulated in Table 4.

#### 4. Conclusions

The  $\text{La}_{3.5}\text{Ru}_4\text{O}_{13}$  and  $\text{La}_2\text{RuO}_5$  compounds were evaluated as possible cathode materials for solid oxide fuel cell. According to the TGA measurements,  $\text{La}_{3.5}\text{Ru}_4\text{O}_{13}$  is stable in an oxidizing as well as in a neutral atmosphere, while  $\text{La}_2\text{RuO}_5$  is partially reduced to  $\text{La}_{10}(\text{Ru}^{3+})_4(\text{Ru}^{4+})\text{O}_{23}$  in neutral atmosphere. A slight decrease in the size of the  $a$  and  $b$  unit-cell parameters of monoclinic  $\text{La}_2\text{RuO}_5$  was observed after firing in neutral atmosphere. In a reducing atmosphere  $\text{La}_{3.5}\text{Ru}_4\text{O}_{13}$  and  $\text{La}_2\text{RuO}_5$  decomposed into metallic Ru and  $\text{La}_2\text{O}_3$ . The thermal expansion coefficients at 800 °C for  $\text{La}_2\text{RuO}_5$  is  $11.2 \times 10^{-6} \text{ K}^{-1}$  and for  $\text{La}_{3.5}\text{Ru}_4\text{O}_{13}$  is  $9.3 \times 10^{-6} \text{ K}^{-1}$ . As compared to the resistivity of  $\text{La}_{3.5}\text{Ru}_4\text{O}_{13}$  ( $2 \times 10^{-2} \Omega$  cm), which is relatively independent of temperature throughout the whole measured temperature range, the specific resistivity of  $\text{La}_2\text{RuO}_5$  decreases with increasing temperature and is 1  $\Omega$  cm at 800 °C.

The stability data in oxidizing atmosphere as well as thermal expansion coefficients of both compounds indicate the possibility to be used as SOFC cathode materials.

## Acknowledgements

The authors would like to thank Dr. Barbara Malič and Ing. Jena Cilenšek for their help with TGA experiments. The financial support of the Ministry of Education, Science and Sport of the Republic of Slovenia is gratefully acknowledged.

## References

- Ralph, J. M., Schoeler, A. C. and Krumpelt, M., Materials for lower temperature solid oxide fuel cells. *J. Mater. Sci.* 2001, **36**, 1161–1172.
- Hammouche, A., Siebert, E. and Hammou, A., Crystallographic, thermal and electrochemical properties of the system  $\text{La}_{1-x}\text{Sr}_x\text{MnO}_3$  for high temperature solid electrolyte fuel cells. *Mater. Res. Bull.* 1989, **24**(3), 367–380.
- Bae, J.-M. and Steele, B. C. H., Properties of pyrochlore ruthenate cathodes for intermediate temperature solid oxide fuel cells. *J. Electroceram.* 1999, **3**(1), 37–46.
- Benčan, A., *Synthesis and Characterization of Lanthanum Ruthenates*. Ph.D. thesis, Faculty of Chemistry and Chemical Technology, University of Ljubljana, 2002.
- Abraham, F., Trehoux, J. and Thomas, D., La liaison metal-metal dans les clusters  $\text{M}_{12}\text{O}_{36}$ : I—preparation et etude structural des phases  $\text{La}_4\text{M}_6\text{O}_{19}$  (M = Ru, Os). *Mater. Res. Bull.* 1997, **12**(1), 43–52.
- Khalifah, P., Nelson, K. D., Jin, R., Mao, Z. Q., Liu, Y., Huang, Q. et al., Non-fermi liquid behavior in  $\text{La}_4\text{Ru}_6\text{O}_{19}$ . *Nature* 2001, **411**, 669–671.
- Abraham, F., Trehoux, J. and Thomas, D.,  $\text{La}_{3.5}\text{Ru}_4\text{O}_{13}$ : un nouveau composé à feuillets de type pérovskite. *J. Solid State Chem.* 1980, **32**(2), 151–160.
- Bouchard, R. J. and Weiher, J. F.,  $\text{La}_x\text{Sr}_{1-x}\text{RuO}_3$ : a new perovskite series. *J. Solid State Chem.* 1972, **4**(1), 80–86.
- Da Costa, F. M., Greatrex, R. and Greenwood, N. N., A study of perovskite solid solution series  $\text{La}_x\text{Sr}_{1-x}\text{RuO}_3$  and  $\text{La}_x\text{Ca}_{1-x}\text{RuO}_3$  by ruthenium-99 Mossbauer spectroscopy. *J. Solid State Chem.* 1977, **20**(4), 381–389.
- Mallika, C. and Sreedharan, O. M., Standard Gibbs energies of formation of  $\text{RuO}_2(\text{s})$  and  $\text{LaRuO}_3(\text{s})$  by oxide e.m.f. measurements. *J. Less Common Metals* 1990, **162**, 51–60.
- Cotton, F. A. and Rice, C. E., The crystal structure of  $\text{La}_3\text{Ru}_3\text{O}_{11}$ : a new cubic  $\text{KSbO}_3$  derivative oxide with no metal-metal bonding. *J. Solid State Chem.* 1978, **2**, 137–142.
- Boullay, Ph., Mercurio, D., Benčan, A., Meden, A., Dražič, G. and Kosec, M., An XRPD ab-initio structural determination of  $\text{La}_2\text{RuO}_5$ . *J. Solid State Chem.* 2003, **170**, 294–302.
- Khalifah, P., Osborn, R., Huang, O., Zandbergen, H. W., Jin, R., Liu, Y. et al., Orbital ordering transition in  $\text{La}_4\text{Ru}_2\text{O}_{10}$ . *Science* 2002, **297**(27), 2237–2240.
- Cotton, F. A. and Rice, C. E., The crystal structure of  $\text{La}_8\text{Ru}_4\text{O}_{21}$ : a mixed-valence ternary ruthenium oxide of a new hexagonal structure type. *J. Solid State Chem.* 1978, **2**, 137–142.
- Khalifah, P., Huang, Q., Ho, D. M., Zandbergen, H. W. and Cava, R. J.,  $\text{La}_7\text{Ru}_3\text{O}_{18}$  and  $\text{La}_{4.87}\text{Ru}_2\text{O}_{12}$ : geometric frustrations in two closely related structures with isolated  $\text{RuO}_6$  octahedra. *J. Solid State Chem.* 2000, **155**, 189–197.
- Khalifah, P., Huang, Q., Lynn, J. W., Erwin, R. W. and Cava, R. J., Synthesis and crystal structure of  $\text{La}_3\text{RuO}_7$ . *Mater. Res. Bull.* 2000, **35**, 1–7.
- Khalifah, P., Erwin, R. W., Lynn, J. W., Huang, Q., Batlogg, B. and Cava, R. J., Magnetic and electronic characterization of quasi—one—dimensional  $\text{La}_3\text{RuO}_7$ . *Phys. Rev. B* 1999, **60**(13), 9573–9578.
- Khalifah, P., Ho, D. M., Huang, Q. and Cava, R. J., The structure and properties of  $\beta\text{-La}_3\text{RuO}_7$ : a new structure type with isolated  $\text{RuO}_6$  octahedra. *J. Solid State Chem.* 2002, **165**, 359–362.
- Stadelmann, P. A., *Ultramicroscopy* 1987, **21**, 131.
- Javoric, S., Dražič, G. and Kosec, M., A study of the crystallization of CSD-prepared  $\text{La}_{(0.5)}\text{Sr}_{(0.5)}\text{Co CO}_3$  thin films using analytical electron microscopy. *J. Eur. Ceram. Soc.* 2001, **21**, 1543–1546.
- Butler, S. R. and Gillson, J. L., Crystal growth, electrical resistivity and lattice parameters of  $\text{RuO}_2$  and  $\text{IrO}_2$ . *Mater. Res. Bull.* 1971, **6**(2), 81–89.